ChemComm

Accepted Manuscript

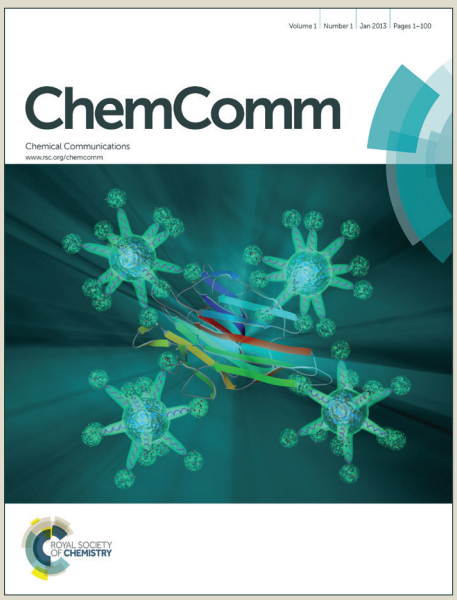

ROYAL SOCIETY OF CHEMISTRY

www.rsc.org/chemcomm

Cite this: DOI: 10.1039/coxx00000x

www.rsc.org/xxxxxx

ARTICLE TYPE

A photothermal cell viability-reporting theragnostic nanoprobe for intraoperative optical ablation and tracking of tumors

Shuqi Wu,[a] Shoufa Han[a,*] Jiahuai Han[b] and Xinhui Su[c,*]

Received (in XXX, XXX) Xth XXXXXXXXX 20XX, Accepted Xth XXXXXXXXX 20XX

DOI: 10.1039/b000000x

A photothermal pH-reporting nanoprobe was developed for intraoperative tumor detection by "turn-on" fluorescence of the probe inside viable tumor cells, photothermal tumor therapy, and in-situ monitoring tumor killing by fluorescence-off of the probe in damaged cells.

Surgical resection is widely used in treatment of solid tumors. Incomplete removal of tumor foci, due to limited visibility of disseminated or tiny tumor foci under visual inspection, results in tumor relapse. As such, optical probes that could guide surgeons to evasive tumor foci are actively explored.[1] Optical systems that could be activated to fluorescence-on states inside tumors while being nonfluorescent in off-target settings are advantageous to achieve high tumor-to-background signal contrast.[2] Probes that could convert light energy into cytotoxic heat are promising tools for photothermal cancer therapy, which is noninvasive and could be administered in a controlled manner with the use of exogenous light.[3] In this contest, near-infrared light (NIR)-absorbing polypyrrole (PPy), displaying a number of favorable characters, is increasingly explored for photothermal therapy.[4] Despite the advances in fluorescence guided staging of evasive tumors, complete surgical removal of small-sized or disseminated tumors remains challenging. As such, alternative modalities that could be use to identify and kill tumors intraoperatively are of clinical significance.

We previously reported the use of acid activatable rhodamine derivatives with intramolecular spiro-rings for fluorescence guided intraoperative detection of tumors in mice by proton triggered turn-on fluorescence within tumors.[5] Herein we report the use of a multifunctional nanoprobe, PPy@SiO_2@dRB, integrating photothermal PPy with acid-responsive *N*-(rhodamine B)-deoxylactam (dRB) for fluorescence guided tumor detection and photothermal killing of tumors (Fig. 1). PPy@SiO_2@dRB features a hydrophilic corona of polyethylene glycol, a silica shell decorated with dRB and an inner core of PPy. Acidic lysosomal pH is maintained in viable cells by V-ATPase mediated proton pumping and is dissipated upon cell death. The fluorescence-off of PPy@SiO_2@dRB within damaged cells due to disruption of lysosomal pH homeostasis was employed for *in situ* monitoring of the photothermal effects on targeted tumors.

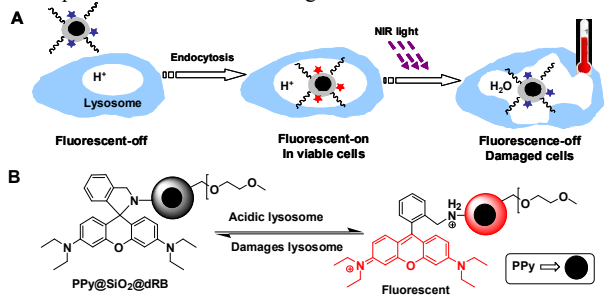

Fig. 1 (A) Illustration of fluorescence guided tumor detection, photothermal destruction and tracking of responses of tumors with PPy@SiO_2@dRB. (B) Surface-anchored dRB isomerizes into fluorescent species within acidic lysosomes and reverts to nonfluorescent state upon loss of lysosomal acidity in cell death.

Light is non-invasive and can be manipulated for biomedical applications in a spatio-temporally controlled manner. Given the limited tissue penetration of external light, we envision that the combination of phototherapy with tumor surgery would be of practical utility owing to exposure of tumor-bearing tissues that are otherwise inaccessible to light. As biological tissues are of the least absorption in NIR region, NIR-absorbing PPy was used as the photothermal agent to conjugate with pH-responsive dRB for fluorescence guided tumor detection. As PPy is a fluorescence quencher, it is critical that conjugated dRB remains emissive within cells. To physically separate PPy and dRB, nanoscaled PPy prepared by ferric chloride mediated polymerization[6] was first coated with a silica shell via condensation with tetraethoxysilane to give PPy@SiO_2 which was further functionalized with dRB conjugated triethoxysilane (dRB-PTS) and 3-aminopropyltriethoxysilane (APTS) to introduce dRB profluorophore and amino moieties on the surface (Scheme S1, ESI†). To increase the colloidal stability and decrease *in vivo* recognition by the reticuloendothelial systems, the as-prepared particles were modified with polyethylene glycol to afford PPy@SiO_2@dRB which was used for *in vitro* cell studies and *in vivo* tumor targeting.

Scanning electron microscopic (SEM) images show that PPy@SiO_2@dRB is of uniform diameter of 100 nm whereas that of PPy is 50 nm (Fig. 2A), which is consistent with dynamic light scattering analysis (Fig. S1, ESI †). Zeta potential analysis showed that the surface potentials decreased from 6.9 mV to -3.8 mV after pegylation of PPy@SiO_2@dRB (ESI†, Fig S2). These results confirm the formation of silica shells around PPy. To probe its pH responsiveness, PPy@SiO_2@dRB was spiked into buffers of various pH and the fluorescence emission was recorded over buffer pH. As shown in Fig. 2B, PPy@SiO_2@dRB, weakly fluorescent at neutral or alkaline conditions, exhibits strong emission centered at 590 nm which intensifies as the buffer pH decreases. The pKa of dRB entity was estimated to be 6.5. Analysis of the solutions by UV-vis-NIR spectroscopy showed that PPy@SiO_2@dRB displays characteristic absorbance of rhodamine B under acidic pH (Fig. 2C), further proving the presence of dRB on silica shells. Compared with SiO_2@dRB devoid of PPy, PPy@SiO_2@dRB displays significant absorbance

in 650-900 nm (Fig. 2D), suggesting its capability to absorb NIR light. Aqueous solutions spiked with various amounts of PPy@SiO_2@dRB were exposed to 808-nm laser illumination at the power density of 2 W cm^{-2}. The solutions displayed dose- and irradiation time-dependent temperature elevation (Fig. 2E), showing PPy@SiO_2@dRB effectively convert NIR light into heat.

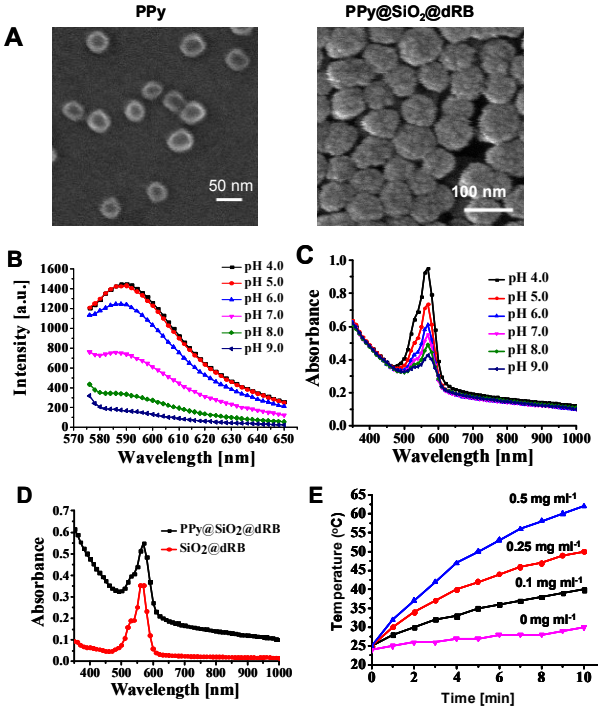

Fig. 2 Characterization of PPy@SiO_2@dRB. (A) SEM images of PPy and PPy@SiO_2@dRB; (B) fluorescence emission of PPy@SiO_2@dRB (50 μg ml^{-1}) in sodium-phosphate buffer (pH 4.0-9.0) (λex@560 nm); (C) UV-vis-NIR absorption spectra of PPy@SiO_2@dRB (50 μg ml^{-1}) in sodium-phosphate buffer (pH 4.0-9.0); (D) UV-vis-NIR absorption of PPy@SiO_2@dRB (50 μg ml^{-1}) and SiO_2@dRB (50 μg ml^{-1}) in sodium-phosphate buffer (pH 7.0); (E) the temperature of water containing PPy@SiO_2@dRB (0-0.5 mg ml^{-1}) upon irradiation with NIR laser (808 nm, 2 W).

Lysosomes are acidic subcellular vesicles where the acidity is maintained in viable cells by V-ATPase mediated pumping of proton into lysosomes driven by ATP hydrolysis. To probe lysosomal pH mediated fluorescence, HeLa, HepG2 and 4T1 cells were respectively cultured with PPy@SiO_2@dRB in medium spiked with LysoTracker Green DND-26 (referenced to as Lysotracker green). No obvious fluorescence was identified in cells or culture medium right after addition of PPy@SiO_2@dRB. Upon incubation, confocal microscopic images show that rhodamine fluorescence is clearly identified within all the cell lines tested and colocalizes with Lysotracker green which is a lysosome specific dye (Fig. 3), showing that the probe becomes fluorescent upon internalization into lysosomes. To access the effects of lysosomal acidity on dRB fluorescence, we acquired signals of PPy@SiO_2@dRB in cells treated with Bafilomycin A1 (BFA) which inhibits the activity of V-ATPase and alkalinizes lysosomal pH.[7] The intracellular fluorescence largely vanished in BFA-treated cells (Fig. 3), confirming lysosomal acidity dependent "turn-on" signal of PPy@SiO_2@dRB within cells.

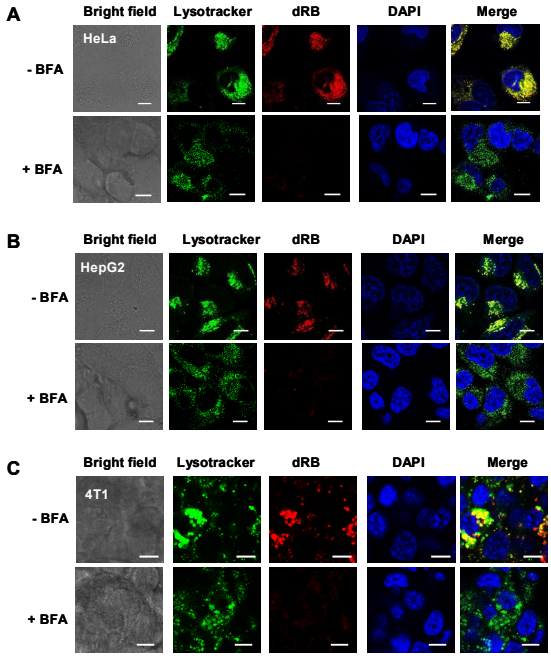

Fig. 3 Lysosomal pH dependent fluorescence of PPy@SiO_2@dRB. HeLa (A), HepG2 (B) and 4T1 cells (C) treated with or without BFA (50 nM) were respectively cultured in Dulbecco's modified Eagle's medium (DMEM) supplemented with PPy@SiO_2@dRB (50 μg ml^{-1}) and DAPI (1 μM) for 2 h and then stained with Lysotracker green (1 μM) for 30 min. The cells were visualized by confocal fluorescence microscopy. Colocalization revealed by overlay of dRB signals (shown in red) with Lysotracker green signals (shown in green) was indicated by the yellow areas. Bars, 5 μm.

Demonstrated to be luminescent within acidic lysosomes, PPy@SiO_2@dRB was evaluated for its feasibility to report cell death. HeLa, 4T1 and HepG2 cells were respectively cultured with PPy@SiO_2@dRB or SiO_2@dRB and then irradiated with or without NIR laser. No obvious fluorescence changes were observed in control cells treated with NIR light and SiO_2@dRB (Fig. S3, ESI†). In contrast, the intracellular fluorescence largely disappeared in all the cell lines treated with PPy@SiO_2@dRB and NIR illumination (Fig. 4), demonstrating PPy dependent fluorescence-off upon NIR irradiation. As dRB fluorescence is dependent on lysosomal acidity (Fig. 3), these results suggest disruption of lysosomal pH by heat generated from NIR laser with the aid of PPy@SiO_2@dRB. Cell viability assay using 3-(4,5-dimethylthiazol-2-yl)-2,5-diphenyltetrazolium (MTT) reveals significant cell death in the three cell lines treated with NIR light and PPy@SiO_2@dRB whereas the viability of cells treated with NIR laser (808 nm, 2 W) or PPy@SiO_2@dRB alone was largely unaffected (Fig. 4E). In control experiments, no detrimental effects were observed on the viability of HeLa, 4T1 and HepG2 cells treated with SiO_2@dRB and NIR irradiation (ESI†, Fig. S3). These results establish the synergistic effects of PPy@SiO_2@dRB and NIR irradiation for effective photothermal killing of targeted cells. Collectively, the NIR irradiation-triggered decrease of intracellular fluorescence validates the use of PPy@SiO_2@dRB for reporting of cell death.

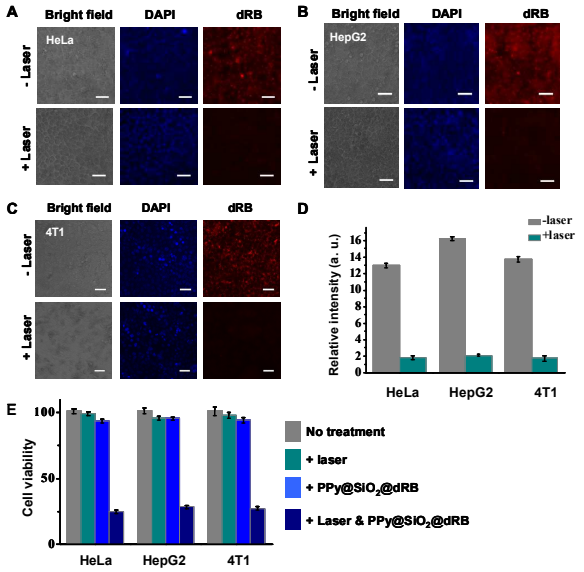

Fig. 4 NIR irradiation-mediated signal-off of PPy@SiO_2@dRB within cells. HeLa (A), HepG2 (B) and 4T1 cells (C) were respectively cultured for 6 h in DMEM spiked with or without PPy@SiO_2@dRB (50 μg ml^{-1}), and then irradiated with or without NIR laser in fresh DMEM for 10 min. The cells were analyzed by fluorescence microscopy and MTT assay; (D) intracellular fluorescence emission of dRB@575-590 nm was collected using *λex*@510-560 nm; (E) cell viability was determined by MTT assay. Bars, 50 μm.

With cell death correlated signal-off of PPy@SiO_2@dRB (Fig. 4), we explored its potentials for intraoperative photothermal tumor therapy in mice models. 4T1 mouse breast carcinoma cells were subcutaneously injected into the flank of female Balb/c mice. Within 5-10 days after xenograft, PPy@SiO_2@dRB and SiO_2@dRB were respectively injected *via* tail vein into the bloodstreams of the tumor-bearing mice. The mice were sacrificed 12 h postinjection and the subcutaneous tumors were dissected and irradiated with NIR laser for 5 min. *Ex vivo* fluorescence images revealed strong rhodamine fluorescence in both subcutaneous tumors from mice treated with PPy@SiO_2@dRB and SiO_2@dRB (Fig. 5), showing that these probes could effectively accumulate and become luminescent in tumors and thus proving their uses for fluorescence-guided intraoperative tumor detection. To our delight, the tumor from mice treated with PPy@SiO_2@dRB displayed marked fluorescence attenuation upon *ex vivo* NIR irradiation whereas no obvious signal changes were observed in the tumor from mice injected with SiO_2@dRB under identical treatment (Fig. 5). The difference clearly validates the feasibility to track photothermal effects on tumors with PPy@SiO_2@dRB during surgery.

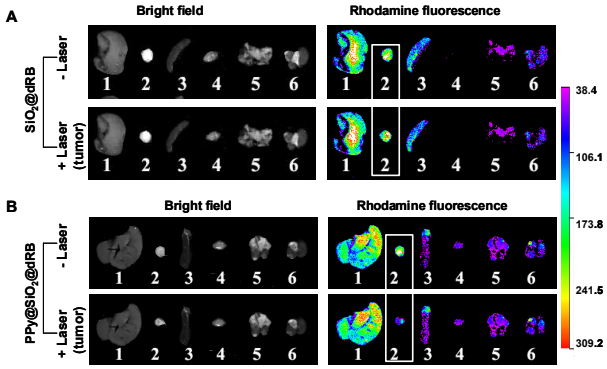

Fig. 5 NIR irradiation mediated fluorescence attenuation of PPy@SiO_2@dRB in subcutaneous tumors. Balb/c mice with subcutaneous tumors were intravenously injected with SiO_2@dRB (30 mg kg^{-1}) (A) or PPy@SiO_2@dRB (30 mg kg^{-1}) (B) via tail vein and then sacrificed 12 h postinjection. The representative organs and tumors were dissected and imaged by *ex vivo* fluorescence analysis. The tumors were illuminated with or without NIR laser for 5 min and then imaged for tumor-associated fluorescence in parallel with organs free of NIR irradiation. The organs are arrayed in the following sequence: liver (1), tumor (2), spleen (3), heart (4), lung (5), and kidney (6).

In summary, photothermal and acid activatable PPy@SiO_2@dRB was prepared and shown to become fluorescent within acidic lysosomes upon cellular internalization. Efficient cell death was induced by NIR irradiation and endocytosed PPy@SiO_2@dRB, leading to fluorescence-off of the probe in cells and subcutaneous tumors owing to heat-triggered loss of functional lysosomal pH in damaged cells. Photothermal PPy@SiO_2@dRB, with cell viability-reporting optical read-out, would be of potential utility for fluorescence-guided intraoperative tumor detection, photothermal killing of surgically exposed tumors, and *in situ* tracking of the effects of photothermal therapy during surgical tumor treatment.

Notes and references

[a]*Department of Chemical Biology, College of Chemistry and Chemical Engineering, the Key Laboratory for Chemical Biology of Fujian Province, The MOE Key Laboratory of Spectrochemical Analysis & Instrumentation, and Innovation Center for Cell Biology, Xiamen University;* [b]*State key Laboratory of Cellular Stress Biology, Innovation Center for Cell Biology, School of Life Sciences, Xiamen University,* [c]*Department of Nuclear Medicine, Zhongshan Hospital, Xiamen University, Xiamen 361005, China; Tel: 86-0592-2181728; E-mail: shoufa@xmu.edu.cn; suxinhuii@163.com*

Acknowledgments: Dr S. Han was supported by grants from 973 program (2013CB93390), NSFC (21272196), the Fundamental Research Funds for the Central Universities (2012121018), NSF of Fujian Province (2011J06004), and PCSIR; Dr X. Su was supported by grants from NSFC (81071182) and Medical Innovation Foundation of Fujian (2009-CXB-46).

† Electronic Supplementary Information (ESI) available on experimental procedures; synthesis and characterization of PPy@SiO_2@dRB and SiO_2@dRB; Effects of NIR irradiation on the fluorescence of SiO_2@dRB within cells; Cytotoxicity of PPy@SiO_2@dRB. See DOI: 10.1039/b000000x/

1 (a) Y. Urano, D. Asanuma, Y. Hama, Y. Koyama, T. Barrett, M. Kamiya, T. Nagano, T. Watanabe, A. Hasegawa, P. L. Choyke, H. Kobayashi, *Nat. Med.,* 2009, **15**, 104; (b) G. M. van Dam, G. Themelis, L. M. Crane, N. J. Harlaar, R. G. Pleijhuis, W. Kelder, A. Sarantopoulos, J. S. de Jong, H. J. Arts, A. G. van der Zee, J. Bart, P. S. Low, V. Ntziachristos, *Nat. Med.,* 2011, **17**, 1315; (c) Q. T. Nguyen, E. S. Olson, T. A. Aguilera, T. Jiang, M. Scadeng, L. G.

Ellies, R. Y. Tsien, *Proc. Natl. Acad. Sci. USA,* 2010, **107**, 4317; (d) Y. Urano, M. Sakabe, N. Kosaka, M. Ogawa, M. Mitsunaga, D. Asanuma, M. Kamiya, M. R. Young, T. Nagano, P. L. Choyke, H. Kobayashi, *Sci. Transl. Med.,* 2011, 3, 110ra119; (e) X. Wu, Y. Tian, M. Yu, B. Lin, J. Han, S. Han, *Biomater. Sci.* 2014, DOI: DOI:10.1039/C4BM00028E

2 (a) H. Kobayashi, P. L. Choyke, *Acc. Chem. Res.,* 2011, **44**, 83; (b) H. Kobayashi, M. Ogawa, R. Alford, P. L. Choyke, Y. Urano, *Chem. Rev.,* 2010, **110**, 2620; (c) H. Lee, W. Akers, K. Bhushan, S. Bloch, G. Sudlow, R. Tang, S. Achilefu, *Bioconjug. Chem.,* 2011, **22**, 777.

3 (a) E. B. Dickerson, E. C. Dreaden, X. Huang, I. H. El-Sayed, H. Chu, S. Pushpanketh, J. F. McDonald, M. A. El-Sayed, *Cancer Lett.,* 2008, **269**, 57; (b) X. Huang, P. K. Jain, I. H. El-Sayed, M. A. El-Sayed, *Lasers Med. Sci.,* 2008, 23, 217; (c) X. Liu, H. Tao, K. Yang, S. Zhang, S. T. Lee, Z. Liu, *Biomaterials,* 2011, **32**, 144; (d) X. Huang, I. H. El-Sayed, W. Qian, M. A. El-Sayed, *J. Am. Chem. Soc.,* 2006, **128**, 2115; (e) K. Yang, S. Zhang, G. Zhang, X. Sun, S. T. Lee, Z. Liu, *Nano. Lett.,* 2010, **10**, 3318; (f) L. R. Hirsch, R. J. Stafford, J. A. Bankson, S. R. Sershen, B. Rivera, R. E. Price, J. D. Hazle, N. J. Halas, J. L. West, *Proc. Natl. Acad. Sci. USA.,* 2003, **100**, 13549; (g) J. Chen, C. Glaus, R. Laforest, Q. Zhang, M. Yang, M. Gidding, M. J. Welch, Y. Xia, *Small,* 2010, **6**, 811; (h) J. Yang, J. Choi, D. Bang, E. Kim, E. K. Lim, H. Park, J. S. Suh, K. Lee, K. H. Yoo, E. K. Kim, Y. M. Huh, S. Haam, *Angew. Chem. Int. Ed.,* 2011, **50**, 441; (i) J. Zhou, Z. Lu, X. Zhu, X. Wang, Y. Liao, Z. Ma, F. Li, *Biomaterials,* 2013, **34**, 9584.

4 (a) M. Chen, X. Fang, S. Tang, N. Zheng, *Chem. Commun.,* 2012, **48**, 8934; (b) K. Yang, H. Xu, L. Cheng, C. Sun, J. Wang, Z. Liu, *Adv. Mater.,* 2012, **24**, 5586; (c) Z. Zha, X. Yue, Q. Ren, Z. Dai, *Adv. Mater.,* 2013, **25**, 777.

5 (a) Z. LI, Y. Song, Y. Yang, L. Ynag, X. Huang, J. Han, S. Han, *Chem. Sci.,* 2012, **3**, 2941; (b) X. Wu, Y. Tian, M. Yu, J. Han, S. Han, *Biomater. Sci.* 2014, DOI: 10.1039/C1034BM00007B

6 J. Y. Hong, H. Yoon, J. Jang, *Small,* 2010, **6**, 679.

7 T. Yoshimori, A. Yamamoto, Y. Moriyama, M. Futai, Y. Tashiro, *J. Biol. Chem.,* 1991, **266**, 17707.